Sampling and Recovery of Binary Shapes via Low-Rank structures

Saeed Razavikia, Hojatollah Zamani, and Arash Amini
EE Department, Sharif University of Technology. Tehran, Iran
Email: {saeedrazavikia, hojatollah.zamani}@ee.sharif.edu, aamini@sharif.edu

***Abstract*—The binary-valued images usually represent shapes. Therefore, the recovery of binary images from samples is often linked with recovery of shapes, where certain parametric structures are assumed on the shape. In this paper, we study the recovery of shape images with the perspective of low-rank matrix recovery. The matrix of such images is not automatically low-rank. Therefore, we consider the Hankel transformation of binary images in order to apply tools in low-rank matrix recovery. We introduce an ADMM technique for the reconstruction which is numerically confirmed to yield suitable results. We also analyze the sampling requirement of this process based on the theory of random matrices.**

I. Introduction

Shape images or binary-valued images are an important part of various applications such as medical imaging [1], millimiter-wave imaging [2], shape processing [3], and image segmentation [4]. The imaging devices, due to physical constraints, usually convert these shapes into multi-level pixel values (samples). Effectively, one can model the imaging process as a convolution (with the point-spread function) followed by sampling. Now, the recovery task is to retrieve the sharp binary image based on the blurred samples.

The framework of signals with finite rate of innovation (introduced in [5] and further developed in [6] for 1D signals) has been a frequent tool in studying the shape images recently. The shape images with bandlimited periodic boundaries are studied in [7], where the Fourier coefficients of the boundary curve are recovered by the annihilation filter of the FRI framework. A related problem appeared in [8], where the shape boundaries are assumed to be algebraic curves. The annihilation filter technique is then used to estimate the coefficients of the underlying polynomial. Piecewise constant images with trigonometric boundaries are studied in [9]; the task is to recover the image from low-pass Fourier samples.

The recovery of piece-wise constant images was recently investigated in [10] using a combination of low-rank matrix recovery and annihilation equations. Indeed, a link between 1D FRI signals and low-rank matrices were previously established in [11] based on the work of [12] in recovering spectrally sparse signals via low-rank models.

The convolution part of the sampling process has a great impact in the overal performance of the image recovery. In [13], the blind recovery of the convolution kernel is considered. The goal is to simultaneously recover the kernel and the image based on the uniform samples. For this purpose, both the image and the kernel are assumed to belong to a low-dimensional space, and the sampling pattern is taken as random. In this paper, we combine the discrete model of [13] with the sampling model of [8]; more precisely, we assume to know the convolution kernel and apply a uniform sampling strategy. Unlike most previous works in shape image recovery, we do not use a parametric model for the shape boundaries. In order to reconstruct the image, we first reformulate the model using the concatenated block low-rank Hankel structure introduced in [12]. Then, we propose an ADMM technique for the recovery.

II. Model and Sampling

In this work, we consider a discrete bi-level (black and white) image of size $N \times N$ with shape $\mathcal{S}$ defined as

$$I[m,n] = \begin{cases} 1, & [m,n] \in \mathcal{S} \\ 0, & [m,n] \in \Omega/\mathcal{S} \end{cases} \tag{1}$$

where $\Omega = [N] \times [N]$ is the image plane. We represent boundaries of the shape with $\partial\mathcal{S}$. The image $\boldsymbol{I} \in \{0,1\}^{N\times N}$ is convolved with a low-pass kernel [1] of size $L \times L$ represented by $\{\varphi(i,j)\}_{i=1,j=1}^{L,L}$. So, the resulting image after filtering has the elements

$$d_{i,j} = \sum_{\Omega}\sum_{\Omega} I[m,n]\varphi\big[m-i, n-j\big] \tag{2}$$
$$\forall i = \big[\tfrac{L_1}{2}+1, N+\tfrac{L_1}{2}\big], j = \big[\tfrac{L_2}{2}+1, N+\tfrac{L_2}{2}\big],$$

which forms the matrix $\boldsymbol{D} = [d_{i,j}] \in \mathbb{R}^{N\times N}$. In the sampling process, we only observe a subset $\Omega_d \in [N] \times [N]$ of $\boldsymbol{D}$. Our aim is to recover the binary image $\boldsymbol{I} \in \{0,1\}^{N\times N}$ from samples Ω_d of $\boldsymbol{D}$. Figure 1 depicts a schematic diagram of this process. This means that we can show the resulting sampled image $\boldsymbol{R}$ by

$$\mathbf{R} = \mathcal{P}_{\Omega_d}(\mathbf{\Phi I \Phi}^T), \tag{3}$$

where $\mathcal{P}_{\Omega_d}$ is the projection operator onto the elements of Ω_d and zeros everywhere else. $\mathbf{\Phi} \in \mathbb{R}^{N\times N}$ is matrix corresponding to the 2-D convolution in (2). We define 2-D Hankel operator $\mathscr{H}(\boldsymbol{X}) \in \mathbb{R}^{d^2\times(N-d+1)^2}$ for any matrix $\boldsymbol{X} \in \mathbb{R}^{N\times N}$ as

$$\mathscr{H}(\boldsymbol{X}) := \begin{bmatrix} \mathfrak{h}(\boldsymbol{X}_1) & \mathfrak{h}(\boldsymbol{X}_2) & \dots & \mathfrak{h}(\boldsymbol{X}_{N-d+1}) \\ \mathfrak{h}(\boldsymbol{X}_2) & \mathfrak{h}(\boldsymbol{X}_3) & \dots & \mathfrak{h}(\boldsymbol{X}_{N-d+2}) \\ \vdots & \vdots & \vdots & \vdots \\ \mathfrak{h}(\boldsymbol{X}_d) & \mathfrak{h}(\boldsymbol{X}_{d+1}) & \dots & \mathfrak{h}(\boldsymbol{X}_N) \end{bmatrix}, \tag{4}$$

[1] In the paper, we will occasionally use the term blurring kernel for this kernel.

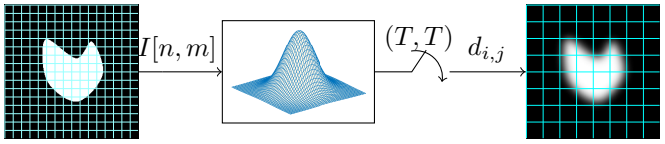

Fig. 1: Sampling scenario, the image are convolved with a 2D kernel followed by sampling to generate the measurements.

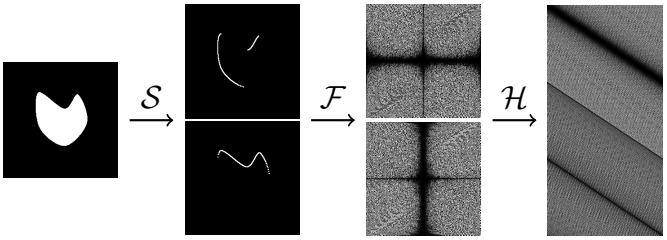

Fig. 2: How to build low rank Hankel structure from a binary image .

where $\mathfrak{h}(\boldsymbol{x}_l)$ for the l-th row $\boldsymbol{x}_l$ of the matrix $\boldsymbol{X}$ is given by

$$\mathfrak{h}(\boldsymbol{x}_l) := \begin{bmatrix} X_{l,1} & X_{l,2} & \dots & X_{l,N-d+1} \\ X_{l,2} & X_{l,3} & \dots & X_{l,N-d+2} \\ \vdots & \vdots & \vdots & \vdots \\ X_{l,d} & X_{l,d+1} & \dots & X_{l,N} \end{bmatrix}, \tag{5}$$

also, d is a scalar from the set $[N]$. We also have pseudo-inverse mapping of Hankel $\mathcal{H}^\dagger : \mathbb{R}^{d^2\times(N-d+1)^2} \to \mathbb{R}^{N\times N}$ which is equivalent taking the average value and putting it back to the original coordinate.

III. Main Results

A. Recovery From Uniform Spatial Samples

According to the presented theory in [12], the rank of Hankel structure of sum of R discrete delta is less than R. The Hankel structure reforms the matrix of data to be a low rank structure. Therefore, if the input signal has sparse representation in spatial domain its Hankel structure will be low rank in the Fourier domain. So, by using the sparsity assumption of the gradients of binary shapes, we build a low rank Hankel structure from image which is shown in Fig 2. In the first step, according to the low rankness of Hankel structure, we reconstruct original image subject to input samples. The Mathematical formulation of the problem is equivalent to

$$\begin{aligned} \underset{\mathbf{g}\in\{0,1\}^{N\times N}}{\text{minimize}} \quad & \operatorname{rank}(\mathcal{H}(\mathbf{g})) \\ \text{subject to} \quad & \mathcal{P}_{\Omega_d}(\mathbf{\Phi}\mathbf{g}\mathbf{\Phi}^T) = \mathbf{D}, \end{aligned} \tag{6}$$

where $\mathcal{H}(\mathbf{g})$ is the block Hankel structure formed by vertically concatenation of the multi Hankel block structure as

$$\mathcal{H}(\mathbf{g}) = \begin{bmatrix} \mathscr{H}\Big(\mathcal{F}\big(\mathcal{W}_1(\mathbf{g})\big)\Big) \\ \mathscr{H}\Big(\mathcal{F}\big(\mathcal{W}_2(\mathbf{g})\big)\Big) \\ \vdots \end{bmatrix} \tag{7}$$

where $\mathscr{H}(\mathbf{g}) \in \mathbb{C}^{d_1\times d_2}$ is a block Hankel structure defined in (4). $\mathcal{F}$ is Fourier transform and $\mathcal{W}_i$ represent i^{th} invertable sparsifying transforms. Note that, the sparse transforms can be various transforms such as gradient, wavelet, etc. transforms. For simplicity, in this article we consider one block Hankel as

$$\mathcal{H}(\mathbf{g}) = \mathscr{H}\Big(\mathcal{F}\big(\mathcal{W}(\mathbf{g})\big)\Big). \tag{8}$$

Due to searching in discrete space and non-convexity of rank function, optimization in (6) is NP-hard. Hence, in order to solve this problem, we relax both feasible set and objective function such that

$$\begin{aligned} \underset{\mathbf{g}\in[0,1]^{N\times N}}{\text{minimize}} \quad & \|\mathcal{H}(\mathbf{g})\|_* \\ \text{subject to} \quad & \mathcal{P}_{\Omega_d}(\mathbf{\Phi}\mathbf{g}\mathbf{\Phi}^T) = \mathbf{D} \end{aligned} \tag{9}$$

where $\|\cdot\|_*$ denotes the nuclear norm (or sum of the singular values of the matrix) which is the convex relaxation of the rank function. Equation (9) is a convex problem and it can be efficiently solved by several methods.

B. Algorithm

In order to solve Hankel structured matrix recovery problem from pixelized images, we employ an SVD free structured rank minimization algorithm. The algorithm is based on the following

$$\|\mathbf{A}\|_* = \underset{\mathbf{U},\mathbf{V}\in\mathbb{C}^{R\times N}\mathbf{A}=\mathbf{U}\mathbf{V}^*}{\text{minimize}} \|\mathbf{U}\|_F^2 + \|\mathbf{V}\|_F^2 \tag{10}$$

Therefore it can be reformulated as the nuclear norm minimization problem under the matrix factorization constraint as

$$\begin{aligned} \underset{\mathbf{U},\mathbf{V},\mathcal{H}(\mathbf{g})=\mathbf{U}\mathbf{V}^*,\mathbf{g}\in[0,1]^{N\times N}}{\text{minimize}} \quad & \|\mathbf{U}\|_F^2 + \|\mathbf{V}\|_F^2 \\ \text{subject to} \quad & \tilde{\mathbf{\Phi}}\mathbf{g}\tilde{\mathbf{\Phi}}^T = \mathbf{D} \end{aligned} \tag{11}$$

where $\tilde{\mathbf{\Phi}}$ is the matrix $\mathbf{\Phi}$ restricted to the rows indexed by the first elements of Ω_d. For solving (11), we employ alternating direction method of multiplier (ADMM) technique. By combining the two constraints, we have the following Lagrangian cost function

$$\begin{aligned} &\mathcal{L}(\mathbf{U},\mathbf{V},\mathbf{g},\boldsymbol{\lambda}_1,\boldsymbol{\lambda}_2) := \frac{1}{2}(\|\mathbf{U}\|_F^2 + \|\mathbf{V}\|_F^2) \\ &+ \frac{\mu_1}{2}\|\mathcal{H}(\mathbf{g}) - \mathbf{U}\mathbf{V}^* + \boldsymbol{\lambda}_1\|_F^2 + \frac{\mu_2}{2}\|\tilde{\mathbf{\Phi}}\mathbf{g}\tilde{\mathbf{\Phi}}^T - \mathbf{D} + \boldsymbol{\lambda}_2\|_F^2 \end{aligned}$$

Now, $\mathbf{g}^{(k+1)}$,$\mathbf{U}^{(k+1)}$, and $\mathbf{V}^{(k+1)}$ can be obtained by sequentially applying the following alternative optimization problems

$$\begin{aligned} \mathbf{g}^{(k+1)} = &\underset{\mathbf{g}\in[0,1]^{N\times N}}{\arg\min} \frac{\mu_1}{2}\|\mathcal{H}(\mathbf{g}) - \mathbf{U}\mathbf{V}^* + \boldsymbol{\lambda}_1^{(k)}\|_F^2 \\ &+ \frac{\mu_2}{2}\|\mathbf{D} - \tilde{\mathbf{\Phi}}\mathbf{g}\tilde{\mathbf{\Phi}}^T + \boldsymbol{\lambda}_2^{(k)}\|_F^2, \end{aligned} \tag{12}$$

$$\begin{aligned} \mathbf{U}^{(k+1)} = &\arg\min_{\mathbf{U}} \frac{1}{2}\|\mathbf{U}\|_F^2 \\ &+ \frac{\mu_1}{2}\|\mathcal{H}(\mathbf{g}^{(k+1)}) - \mathbf{U}\mathbf{V}^{*(k)} + \boldsymbol{\lambda}_1^{(k)}\|_F^2, \end{aligned} \tag{13}$$

$$\begin{aligned} \mathbf{V}^{(k+1)} = &\arg\min_{\mathbf{V}} \frac{1}{2}\|\mathbf{V}\|_F^2 \\ &+ \frac{\mu_1}{2}\|\mathcal{H}(\mathbf{g}^{(k+1)}) - \mathbf{U}^{(k+1)}\mathbf{V}^* + \boldsymbol{\lambda}_1^{(k)}\|_F^2. \end{aligned} \tag{14}$$

and the update of Lagrangian multipliers is given by

$$\begin{aligned}\boldsymbol{\lambda}_1^{(k+1)} =&\boldsymbol{\lambda}_1^{(k)} + \mathcal{H}(\mathbf{g}^{(k+1)}) - \mathbf{U}^{(k+1)}\mathbf{V}^{(k+1)*},\\ \boldsymbol{\lambda}_2^{(k+1)} =&\boldsymbol{\lambda}_2^{(k)} + \mathbf{D} - \tilde{\mathbf{\Phi}}\mathbf{g}^{(k+1)}\tilde{\mathbf{\Phi}}^T.\end{aligned} \tag{15}$$

Next, the subproblem for $\mathbf{g}$, $\mathbf{U}$, and $\mathbf{V}$ can be calculated by taking the derivative with respect to each variable. Hence,

$$\begin{aligned}\mathbf{g}^{(k+1)} =&\mathcal{J}^{-1}\Big(\mu_1\mathcal{H}^*(\mathbf{U}\mathbf{V}^* - \boldsymbol{\lambda}_1^{(k)}) + \mu_2\tilde{\mathbf{\Phi}}^T(\mathbf{D} + \boldsymbol{\lambda}_2^{(k)})\tilde{\mathbf{\Phi}}\Big),\\ \mathbf{g}^{(k+1)} =&\mathcal{P}_{[0,1]}(\mathbf{g}^{(k+1)}),\end{aligned} \tag{16}$$

where the linear operators $\mathcal{J} : \mathbb{C}^{N\times N} \mapsto \mathbb{C}^{N\times N}$ is defined as

$$\mathcal{J}(\boldsymbol{X}) = \mu_1\mathcal{H}^*\mathcal{H}(\boldsymbol{X}) + \mu_2\tilde{\mathbf{\Phi}}^T\tilde{\mathbf{\Phi}}\boldsymbol{X}\tilde{\mathbf{\Phi}}\tilde{\mathbf{\Phi}}^{\mathrm{T}}. \tag{17}$$

Also, the mapping operator $\mathcal{P}_{[0,1]}$ would map the result on [0,1] i.e

$$\mathcal{P}_{[0,1]}(\mathbf{Z}) = \begin{cases}1 & Z_{i,j} > 1\\ Z_{i,j} & 1 \geq Z_{i,j} \geq 0\\ 0 & Z_{i,j} < 0\end{cases}$$

Next for $\mathbf{U}$ and $\mathbf{V}$ we have

$$\begin{aligned}\mathbf{U}^{(k+1)} = \mu_1\big(\mathcal{H}(\mathbf{g}^{(k+1)}) + \boldsymbol{\lambda}_1^{(k)}\big)\mathbf{V}^{(k)}.\\ \big(\mathbf{I}_N + \mu_1\mathbf{V}^{*(k)}\mathbf{V}^{(k)}\big)^{-1},\end{aligned} \tag{18}$$

$$\begin{aligned}\mathbf{V}^{(k+1)} = \mu_1\big(\mathcal{H}(\mathbf{g}^{(k+1)}) + \boldsymbol{\lambda}_1^{(k)}\big)\mathbf{U}^{(k+1)}.\\ \big(\mathbf{I}_N + \mu_1\mathbf{U}^{*(k+1)}\mathbf{U}^{(k+1)}\big)^{-1},\end{aligned} \tag{19}$$

where $\mathbf{I}_N$ represent a identity matrix with size $N \times N$. The initialize value of $\mathbf{g}^{(0)}$ is came from the least square problem i.e.

$$\mathbf{g}^{(0)} = \underset{\boldsymbol{X}\in\mathbb{R}^{N\times N}}{\operatorname{argmin}} \|\tilde{\mathbf{\Phi}}(\boldsymbol{X} - \mathbf{I})\tilde{\mathbf{\Phi}}^{\mathrm{T}}\|_{\mathrm{F}}^2 \tag{20}$$

which equals to $\mathbf{g}^{(0)} = \tilde{\mathbf{\Phi}}^{\dagger}\mathbf{D}\tilde{\mathbf{\Phi}}^{\dagger T}$. Then, $\mathbf{U}^{(0)}$ and $\mathbf{V}^{(0)}$ can be computed by the polar decomposition of $\mathcal{H}(\mathbf{g}^{(0)}) = \mathbf{U}\mathbf{V}^{\mathrm{T}}$. Also, we set $\boldsymbol{\lambda}_1^{(0)} = \emptyset$ $\boldsymbol{\lambda}_2^{(0)} = \emptyset$. The converge analyses of ADMM algorithm for minimizing the sum of multi non-smooth convex separable function have been studied in [14] and showed that if the penalty parameter is chosen to be sufficiently large the classical ADMM converges to the set of stationary solutions.

C. Sufficient Number of Samples for Perfect Recovery

In this subsection, we will discuss how to obtain the required number of samples for perfect recovery with a high probability. In [12], the incoherence property is defined which is dependent on relative locations of the frequencies. [10] showed that this property can be related to the geometry of 2-D curves. Similarly, our results depend on an incoherence measure which is derived from the locations of the frequencies and the rows of the matrix $\mathbf{\Phi}$. In fact, if the transform matrix $\mathbf{\Phi}$ be an identity matrix, then this parameter is equal to incoherence measure defined in [10]. First we define the Dirichlet kernel as

$$\mathcal{D}(k_1, k_2, \boldsymbol{r}) := \frac{N^2}{d^2}\Big(\frac{1 - e^{\frac{j2\pi d r_1}{N}}}{1 - e^{\frac{j2\pi r_1}{N}}}\Big)\Big(\frac{1 - e^{\frac{j2\pi d r_2}{N}}}{1 - e^{\frac{j2\pi r_2}{N}}}\Big) \tag{21}$$

where $\boldsymbol{r} = (r_1, r_2) \in [N] \times [N]$. We defined also the Gram matrices $\boldsymbol{G}_L = \mathcal{D}(d, \boldsymbol{r}_i - \boldsymbol{r}_j)$ and $\boldsymbol{G}_R = \mathcal{D}(N-d+1, \boldsymbol{r}_i - \boldsymbol{r}_j)$ as where $\boldsymbol{r}_i$ and $\boldsymbol{r}_j$ are two-dimensional vectors on the image boundary $\partial\mathcal{S}$.

Definition 1: For image $I[m, n]$ with Hankel structure $\mathcal{H}(\mathbf{I})$ and rank R, the incoherence property is defined as

$$\rho_1 = \max\left\{\frac{1}{\sigma_{min}(\mathbf{G}_L)}, \frac{1}{\sigma_{min}(\mathbf{G}_R)}\right\} \tag{22}$$

for all $(i, j) \in [N] \times [N]$. Also, $\boldsymbol{\phi}_{ci}^I$ denotes the ith column of $\mathbf{\Phi}^{-1}$ and $\boldsymbol{\phi}_{ri}$ is the ith row of $\mathbf{\Phi}$.

Definition 2: For the transform matrix $\mathbf{\Phi}$, the kernel parameter ρ_2 is defined as the smallest number that satisfies

$$\rho_2 \geq \max_{(i,j)\in[N]\times[N]}\Bigg\{\|\mathcal{H}^{\dagger *}(\boldsymbol{\phi}_{ri}\boldsymbol{\phi}_{rj}^T)\|_F^2\|\mathcal{H}(\boldsymbol{\phi}_{ci}^I\boldsymbol{\phi}_{cj}^{IT})\|_F^2, \tag{23}$$

$$\|\mathcal{H}^{\dagger *}(\boldsymbol{\phi}_{ri}\boldsymbol{\phi}_{rj}^T)\|^2\|\mathcal{H}(\boldsymbol{\phi}_{ci}^I\boldsymbol{\phi}_{cj}^{IT})\|_1^2\Bigg\} \tag{24}$$

where $\|.\|$ denotes operator norm and $\|.\|_1$ is vector norm 1i.e. the sum of the matrix elements.

Before presenting our main results, we express problem (9) in random scenario as the following

$$\begin{aligned}\underset{\mathbf{g}\in[0,1]^{N\times N}}{\text{minimize}} \quad & \|\mathcal{H}(\mathbf{g})\|_*\\ \text{subject to} \quad & \mathcal{P}_{\Omega_r}(\mathbf{\Phi}\mathbf{g}\mathbf{\Phi}^T) = \mathcal{P}_{\Omega_r}(\mathbf{\Phi}\mathbf{I}\mathbf{\Phi}^T)\end{aligned} \tag{25}$$

where Ω_r is the collection of indices of the observed entries which are picked randomly from $[N] \times [N]$. Precisely, let $\mathcal{H}(\mathbf{g}) = \mathbf{U}\Sigma\mathbf{V}^*$ be singular value decomposition with rank R. Then, the column-wise and row-wise projections of $\mathcal{H}(\mathbf{g})$ are $\mathcal{P}_U(\mathbf{X}) = \mathbf{U}\mathbf{U}^*\mathbf{X}$, $\mathcal{P}_V(\mathbf{X}) = \mathbf{X}\mathbf{V}\mathbf{V}^*$, respectively. We define sampling operator $\mathcal{A}_{i,j} : \mathbb{R}^{d_1\times d_2} \mapsto \mathbb{R}^{d_1\times d_2}$ for every matrix $\mathbf{Z} \in \mathbb{R}^{d_1\times d_2}$ as follows

$$\mathcal{A}_{i,j}(\mathbf{Z}) = \big\langle\mathbf{Z}, \mathcal{H}^{\dagger *}(\boldsymbol{\phi}_{ri}\boldsymbol{\phi}_{rj}^T)\big\rangle\mathcal{H}(\boldsymbol{\phi}_{ci}^I\boldsymbol{\phi}_{cj}^{IT}). \tag{26}$$

Also, the projection operator corresponding to the sample locations can be defined as

$$\mathcal{A}_{\Omega_r}(\mathbf{Z}) = \sum_{(i,j)\in\Omega_r}\big\langle\mathbf{Z}, \mathcal{H}^{\dagger *}(\boldsymbol{\phi}_{ri}\boldsymbol{\phi}_{rj}^T)\big\rangle\mathcal{H}(\boldsymbol{\phi}_{ci}^I\boldsymbol{\phi}_{cj}^{IT}) \tag{27}$$

Hence, the recovery of $\mathbf{I}$ can be reformulated as a matrix recovery problem in the lifted domain. The orthogonal projection to Hankel structure matrices is represented by $\mathcal{A}^{\perp}(\mathbf{X}) = \mathcal{I} - \mathcal{A}(\mathbf{X})$ with identity operator $\mathcal{I}$. Since matrix $\mathcal{H}(\mathbf{I})$ is Hankel structured, $\mathcal{A}^{\perp}\big(\mathcal{H}(\mathbf{I})\big) = 0$. Then, (25) can be reformulated as

$$\begin{aligned}\text{minimize} \quad & \|\mathbf{X}\|_*\\ \text{subject to} \quad & \mathcal{A}_{\Omega_r}(\mathbf{X}) = \mathcal{A}_{\Omega_r}\big(\mathcal{H}(\mathbf{I})\big)\\ & \mathcal{A}^{\perp}(\mathbf{X}) = \mathcal{A}^{\perp}\big(\mathcal{H}(\mathbf{I})\big) = 0.\end{aligned} \tag{28}$$

To obtain exact recovery of convex optimization, it suffices to produce an appropriate dual certificate and to ensure that the norms of the projections $\mathcal{P}_U\big(\mathcal{A}_{(i,j)}\big)$ and $\mathcal{P}_V\big(\mathcal{A}_{(i,j)}\big)$ are bounded. These conditions are stated in following lemma

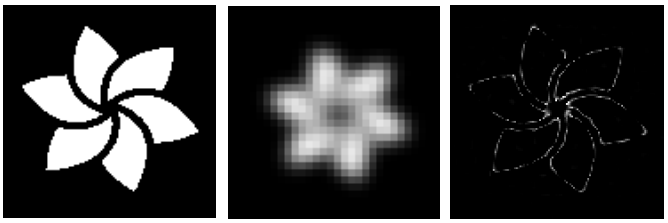

(a) (b) (c)

Fig. 3: Reconstruction of a binary shape. (a) Original Shape, (b) samples (size 30×30) (c) absolute difference between the original shape and recovered (PSNR = 23.06 dB).

Lemma 1: Let $\mathcal{H}(\mathbf{I})$ be the Hankel structure of image $\mathbf{I}$ with rank R and ρ_1 and ρ_2 be incoherence properties of $\mathbf{I}$. then we have

$$\max_{(i,j)\in[N]\times[N]} \{\|\mathbf{U}^* \mathcal{A}_{(i,j)}\|^2, \|\mathcal{A}_{(i,j)}\mathbf{V}\|^2\} \leq \frac{\rho_1 \rho_2 c_s R}{N^2}, \quad (29)$$

The sufficient number of samples for perfect recovery with high probability can be achieved by using this upper bound and by employing the approach of building the dual certificate of [15]. The exact number of samples will be calculated in the future work.

IV. Simulation Result

In this section, we simulate the recovery of binary shapes from their samples. The original image is depicted in Fig. 3(a) with a dimension of 120×120 pixels. We employed 31×31 pixels Gaussian filter as the kernel. The measured 30×30 pixels are drawn in Fig.3(b) with sampling rate of 4 pixels. The proposed algorithm successfully reconstructs the shape with PSNR of 23.06 dB. The error of reconstruction is shown in Fig. 3(c). This simulation is repeated for another complex shape in Fig.4.

V. Conclusion

In this paper, the problem of binary shape recovery from its pixelized samples is discussed. In particular, we presented a low rank structure for the model and formulated a convex optimization problem for recovery. Also, we expressed a theoretical guarantee for exact recovery with high probability for the case of satisfied incoherency property. We proposed an algorithm for image recovery by employing the ADMM approach.

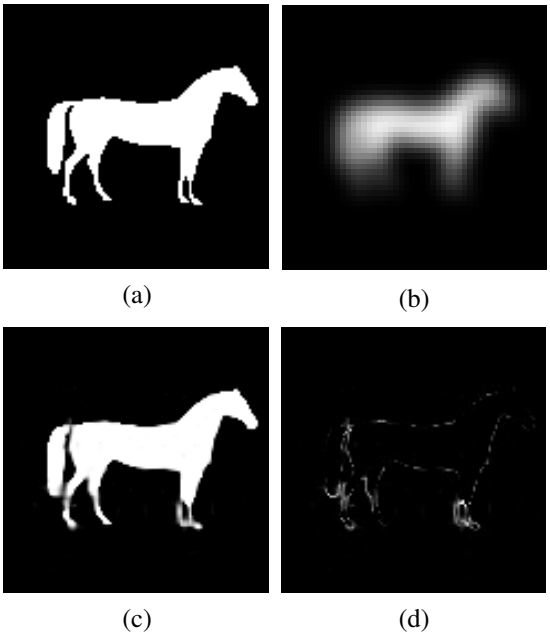

(a) (b) (c) (d)

Fig. 4: Reconstruction of a binary shape. (a) Original Shape, (b) samples (size 50×50) (c) recovery using proposed algorithm (PSNR: 25.48 dB). (d) absolute difference between the original shape and recovered

References

[1] T. Zhang, J. M. Pauly, and I. R. Levesque, "Accelerating parameter mapping with a locally low rank constraint," *Magnetic resonance in medicine*, vol. 73, no. 2, pp. 655–661, 2015.

[2] D. M. Sheen, D. L. McMakin, and T. E. Hall, "Three-dimensional millimeter-wave imaging for concealed weapon detection," *IEEE Transactions on Microwave Theory and Techniques*, vol. 49, no. 9, pp. 1581–1592, Sep. 2001.

[3] M. Fatemi, A. Amini, L. Baboulaz, and M. Vetterli, "Shapes from pixels," *IEEE Transactions on Image Processing*, vol. 25, no. 3, pp. 1193–1206, March 2016.

[4] N. Alajlan, M. S. Kamel, and G. H Freeman, "Geometry-based image retrieval in binary image databases," vol. 30, pp. 1003 – 1013, 07 2008.

[5] M. Vetterli, P. Marziliano, and T. Blu, "Sampling signals with finite rate of innovation," *IEEE transactions on Signal Processing*, vol. 50, no. 6, pp. 1417–1428, 2002.

[6] P. L. Dragotti, M. Vetterli, and T. Blu, "Sampling moments and reconstructing signals of finite rate of innovation: Shannon meets strang–fix," *IEEE Transactions on Signal Processing*, vol. 55, no. 5, pp. 1741–1757, 2007.

[7] H. Pan, T. Blu, and P. L. Dragotti, "Sampling curves with finite rate of innovation," *IEEE Transactions on Signal Processing*, vol. 62, no. 2, pp. 458–471, Jan 2014.

[8] M. Fatemi, A. Amini, and M. Vetterli, "Sampling and reconstruction of shapes with algebraic boundaries," *IEEE Transactions on Signal Processing*, vol. 64, no. 22, pp. 5807–5818, 2016.

[9] G. Ongie and M. Jacob, "Off-the-grid recovery of piecewise constant images from few fourier samples," *SIAM Journal on Imaging Sciences*, vol. 9, no. 3, pp. 1004–1041, 2016.

[10] G. Ongie, S. Biswas, and M. Jacob, "Convex recovery of continuous domain piecewise constant images from nonuniform fourier samples," *IEEE Transactions on Signal Processing*, vol. 66, no. 1, pp. 236–250, 2017.

[11] J. C. Ye, J. M. Kim, K. H. Jin, and K. Lee, "Compressive sampling using annihilating filter-based low-rank interpolation," *IEEE Transactions on Information Theory*, vol. 63, no. 2, pp. 777–801, 2017.

[12] Y. Chen and Y. Chi, "Robust spectral compressed sensing via structured matrix completion," *IEEE Transactions on Information Theory*, vol. 60, no. 10, pp. 6576–6601, 2014.

[13] S. Bahmani and J. Romberg, "Lifting for blind deconvolution in random mask imaging: Identifiability and convex relaxation," *SIAM Journal on Imaging Sciences*, vol. 8, no. 4, pp. 2203–2238, 2015.

[14] M. Hong and Z.-Q. Luo, "On the linear convergence of the alternating direction method of multipliers," *Mathematical Programming*, vol. 162, no. 1-2, pp. 165–199, 2017.

[15] D. Gross, "Recovering low-rank matrices from few coefficients in any basis," *IEEE Transactions on Information Theory*, vol. 57, no. 3, pp. 1548–1566, 2011.